A Review of Substrate Integrated Waveguide End-Fire Antennas

YUFAN CAO[1], **YANG CAI**[2], **LEI WANG**[3], **(Member, IEEE),**
ZUPING QIAN[1], **(Member, IEEE), AND LEI ZHU**[1]

[1]College of Communications Engineering, Army Engineering University of PLA, Nanjing 210007, China
[2]Department of Electric and Optic Engineering, Space Engineering University, Beijing 101400, China
[3]Institute of Electromagnetic Theory, Hamburg University of Technology, 21079 Hamburg, Germany

Corresponding author: Yang Cai (caiyang_1991@163.com)

ABSTRACT Substrate integrated waveguide (SIW) is a planar waveguide structure, which offers the advantages of low profile, ease of fabrication, low insertion loss, and compatibility with other planar circuits. SIW end-fire antennas have drawn broad interests due to the potential applications in aircraft, missile, and radar systems. However, this planar structure suffers from narrow bandwidth due to severe impedance mismatch at the radiating aperture. Meanwhile, the narrow radiating aperture of SIW end-fire antennas also deteriorates the radiation performance. This paper presents a detailed review upon the most recent research efforts concerning the improvement of antenna performances. They are discussed and classified into three different categories from the aspect of polarization properties: horizontally polarized, vertically polarized, and circularly polarized SIW end-fire antennas. Some practical difficulties for the development of SIW end-fire antennas are pointed out and effective approaches are also provided. A wide variety of antenna examples are presented with respect to theoretical and experimental results.

I. INTRODUCTION

The end-fire antennas are used to launch energy into free space along the direction of antenna extension. The main direction of maximum radiation is parallel with the antenna structure, which illustrates that the directivity is independent on aperture size [1]. Compared with broadside antennas, end-fire antennas provide an excellent low aerodynamic drag profile in practical applications such as high speed aircraft, missile, radar, and etc. End-fire antennas are diverse in shape and formation, including log-periodic antennas, tapered slot antennas, Yagi-Uda antennas, and etc. [2]–[4].

Due to the advantages of high directivity, low profile, and etc., end-fire antennas are widely employed and required in military and commercial applications, such as radars and vehicles communication. They can fulfill many tasks such as direction-finding and long-distance communication systems. When end-fire antennas are designed based on substrate integrated waveguide (SIW) technology, benefits of low cost, low profile, low complexity, and easy integration can be obtained while the constraints in material property and packaging resulted from high frequency are well relieved.

Therefore, due to the booming development of modern wireless communication technologies as well as the increase in communication frequency, SIW-based end-fire antennas are urgently needed in practical applications. On the one hand, SIW-based end-fire antennas have extensive applications in microwave and millimeter wave band. For example, in civilian, with the emergence of 5G communication, driverless vehicles are in rapid development. In order to realize intelligent control, real-time traffic status and geographic location should be updated in real time. Therefore, using SIW end-fire antennas as transceivers will not only maintain the beautiful appearance, but also meet with the requirement of material property in millimeter wave communications. In military field, anti-radiation missile radar is a good case in point. On the other hand, SIW-based end-fire antenna could be used as feed source for the microstrip reflectarray antenna. In order to compensate the drawback of parabolic antenna and phased-array antenna, microstrip reflectarray antenna has been presented and studied. Since the advantages of compactness, light weight, and low cost are future development trend for microstrip reflectarray antenna,

using SIW end-fire antennas as feed source could satisfy the requirement.

According to polarization performance, SIW end-fire antennas can be divided into three categories if the conformed surface is selected to be reference plane, namely the horizontally polarized (HP), vertically polarized (VP), and circularly polarized (CP) SIW end-fire antennas. Due to the narrow radiating aperture, vertically polarized SIW end-fire antennas generally exhibit poor impedance matching and radiating performance. Besides, few horizontally polarized electric field component could propagate inside SIW due to the via-gap, which makes it a great challenge to design dual or circularly polarized SIW end-fire antennas.

Design methods of HP, VP and CP SIW end-fire antennas are introduced in sections II–IV. Section V gives a conclusion and future trends for SIW end-fire antennas.
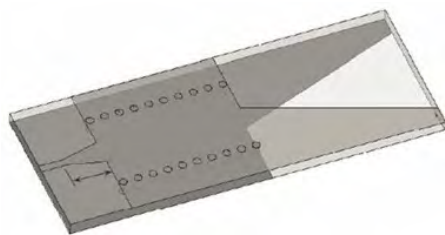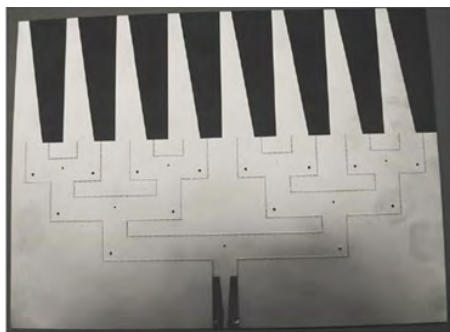

FIGURE 1. Geometry of ALTSA.

FIGURE 2. Geometry of ALTSA array.

II. HP SIW END-FIRE ANTENNAS

The SIW antipodal linearly tapered slot antenna (ALTSA) is one of the most common HP SIW end-fire antennas. In Fig. 1, a feeding system using SIW technique for ALTSA was firstly presented by Hao *et al.* [5]. As for microstrip-like feeding systems, an additional balun structure is used to realize transition from feeding system to radiation structure. However, the SIW is a balanced feeding structure in nature so that the inherently loss can be effectively reduced at high frequency. SIW ALTSAs are widely used in millimeter wave applications due to the advantages of wide bandwidth and high gain. Based on ALTSA element, Cheng designed a series of antenna arrays to expand the applications of SIW end-fire antennas [6], [7], as shown in Fig. 2. Besides, SIW technologies can be adopted in other traditional end-fire antennas such

as Yagi-Uda antennas and log-periodic antennas, and good performances can be obtained [8]–[10].

To sum up, since the phase difference between top and bottom metal pieces of SIW is 180°, SIW can be served as a wideband balun structure to directly feed the end-fire antenna. Meanwhile, the direction of energy propagation is parallel to the horn aperture so that good impedance matching can be realized. Therefore, HP SIW end-fire antennas with high radiation performance are easy to design.

III. VP SIW END-FIRE ANTENNAS

The original VP SIW end-fire antenna was presented by Clénet *et al.* [11], as illustrated in Fig. 3. The VP radiation was realized through an open-ended SIW structure. Meanwhile, a special coaxial-to-waveguide transition was adopted to improve impedance matching and the return loss below −10 dB from 20.2 to 21.3 GHz.
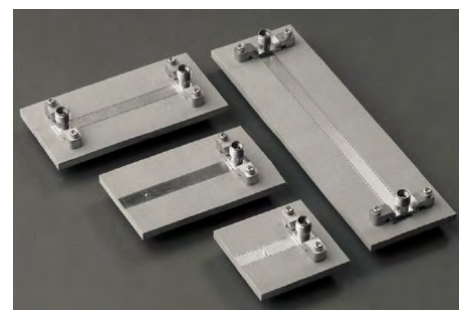

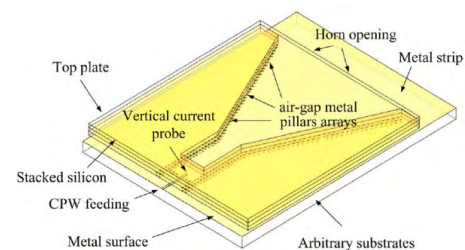FIGURE 3. Geometry of open-ended SIW antenna [11].

FIGURE 4. Geometry of micromachining SIW horn antenna [13].

Wu firstly proposed the SIW horn antenna [12]. A thick foam layer was introduced between the top and bottom substrate to realize large radiating aperture in E-plane. In order to realize good impedance matching on a thin commercial substrate, SIW horn antenna was supposed to be good candidate for millimeter-wave and terahertz applications at the beginning. A 60-GHz coplanar waveguide (CPW) fed SIW horn antenna was presented in [13], as shown in Fig. 4. By adopting surface micromachining technologies and micromachined silicon wafers, high gain and broadband performance was achieved. Meanwhile, antenna efficiency was greatly improved due to the elimination of dielectric loss.

However, above research achievements rely on high accuracy processing technology and special materials, which will not facilitate the development and application of SIW

horn antenna. A series of studies for improving antenna performances and application scenarios of SIW horn antenna sprung up in recent years. According to the design target and primary contribution, these studies can be divided into two categories: broadband SIW horn antenna and high gain SIW horn antenna.

A. BROADBAND SIW END-FIRE ANTENNAS

By loading dielectric lens at the SIW horn aperture on the same single-layer substrate, high gain and narrow beamwidths both in the E-plane and H-plane were obtained [14]. The dielectric lens worked as an impedance transformer and could effectively reduce the mismatch at the horn aperture in some degree. Moreover, the effect of dielectric shapes on impedance matching and radiation performance of SIW horn antenna were further analyzed. Based on this antenna element, 1×4 SIW antenna array and 1×8 SIW monopulse antenna array were fabricated to obtain higher gain. The antenna and array geometries are depicted in Fig. 5.
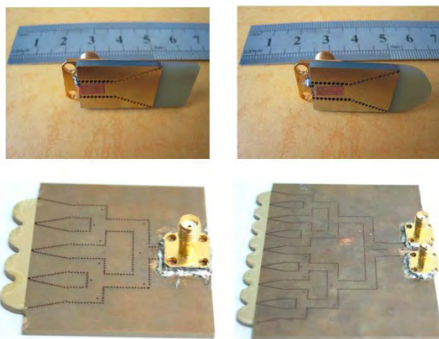

FIGURE 5. Geometry of dielectric-loaded SIW horn antennas and arrays [14].

Another dielectric loaded H-plane SIW horn antenna was proposed in [15]. Unlike the design presented in [14], much thicker Polycarbonate dielectric loading together with metallic strips in front of the SIW horn aperture were applied to improve bandwidth and front-to-back ratio (FTBR). Furthermore, a three-element prototype was fabricated to demonstrate the performance of the proposed design, as shown in Fig. 6.

By introducing low-temperature co-fired ceramic (LTCC) technology into the design of dielectric-loaded SIW horn antenna, a thin SIW-fed network to thick horn transition was realized [16], [17], as shown in Fig. 7.

In Fig. 8(a), a printed transition loaded on a relatively thin substrate was proposed for matching improvement of the SIW horn antenna [18]. Through loading with several rows of metallic blocks on the extended substrate, additional resonant frequencies were generated by the resonant blocks, which made the horn work in a wide band. The great contribution of this research is that commercial substrate can be directly used to build thin SIW horns working well below 20 GHz. Moreover, much wide bandwidth of 16% and high FTBR

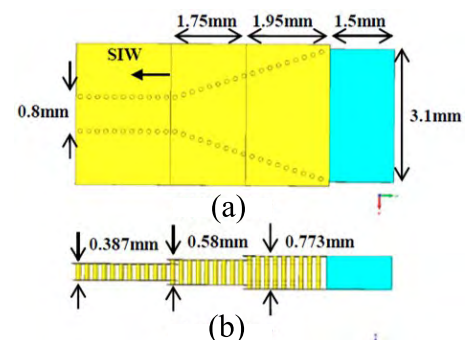**FIGURE 6.** Geometry of Polycarbonate dielectric-loaded SIW horn antenna and array [15].

FIGURE 7. Geometry of dielectric-loaded SIW horn antenna based on LTCC technology [16]. (a) Top view. (b) Side view.

performance were achieved by optimizing the structure of the transition [19], as illustrated in Fig. 8(b). In particular, a circular array of 8 SIW horn antennas was used to provide a full 360° coverage in the azimuthal plane [20].

It is known that the offset double-sided parallel-strip lines (DSPSL) structure owns high characteristic impedance [21]. As shown in Fig. 9, an offset DSPSL structure was loaded in front of the SIW horn antenna with a low profile less than $\lambda_0/13$, leading to good impedance matching and wide bandwidth up to 20.5% [22]. What's more, it provides a flexible transition to improve the impedance matching of SIW horn antenna on a thin substrate.

An H-plane dielectric horn antenna with some periodic parallel strips was proposed [23] and [24]. A width tapering technique was applied in periodic parallel strips to improve matching, as shown in Fig. 10. These strips guide and leak the electromagnetic waves simultaneously enhancing the end-fire radiation characteristics. Finally, an impedance bandwidth up to 40%, a gain of 14.9 dBi at the center frequency, a front-to-back ratio of 33.8 dB, and a side-lobe level of −22.9 dB in the H-plane were achieved.

Due to attractive advantages generated by dielectric loaded structure and printed transition, the two methods were combined together to improve radiation performances of SIW horn antenna [25], [26], as shown in Fig. 11. The printed
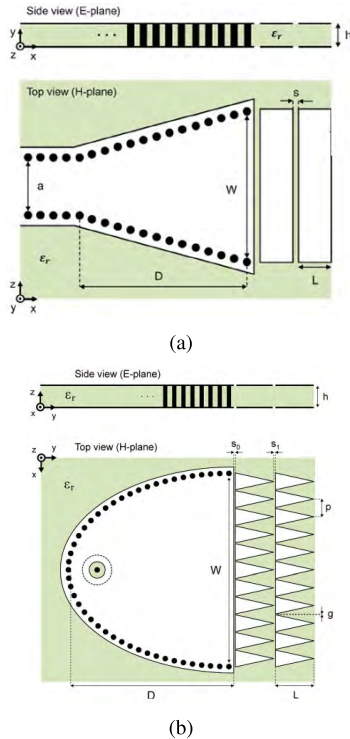
FIGURE 8. Geometry of SIW horn antenna with printed strips. (a) Example [18]. (b) Example [19].
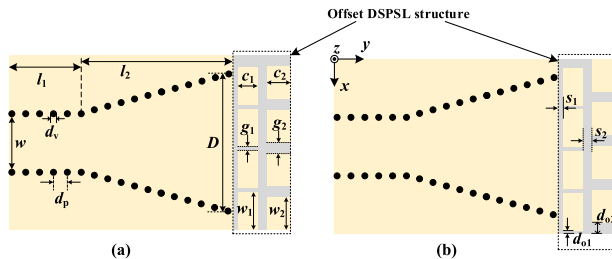

FIGURE 9. Geometry of SIW horn antenna loaded with offset DSPSL structure [22]. (a) Top view. (b) Bottom view.
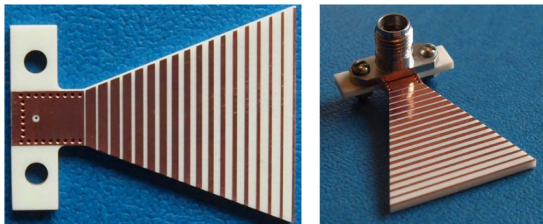

FIGURE 10. Geometry of dielectric horn antenna with periodic parallel strips [23].

FIGURE 11. Geometry of dielectric-loaded SIW horn antenna with printed strips [26].

FIGURE 12. Geometry of SIW horn antenna loaded with air-via perforated dielectric slab. (a) Example [27]. (b) Example [28]. (c) Example [29].

transition improves impedance matching and high FTBR while loaded dielectric increases the gain, respectively.

A stepped impedance transformer was realized through perforating air-vias with different diameters in the extended dielectric [27], as shown in Fig. 12(a). Impedance matching at the horn aperture was greatly improved so that the operating bandwidth could be enlarged to 40%. Besides, size reduction could be realized through adopting the so-called elevated coplanar waveguide (ECPW) feeding structure as
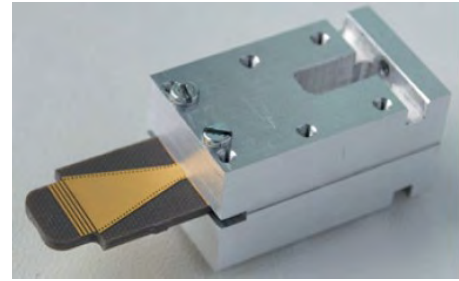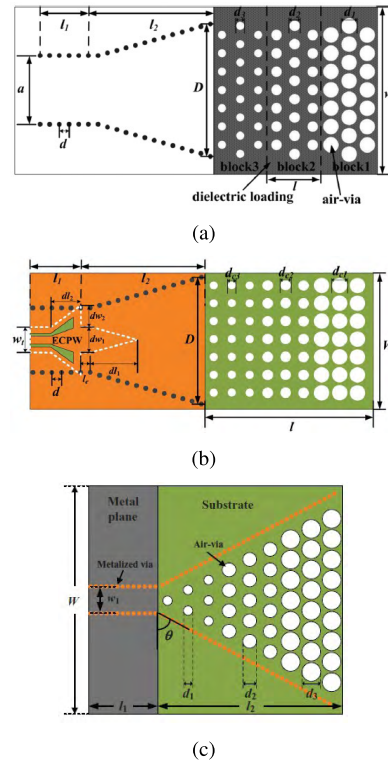
presented in [28] and wideband property was maintained as well, as shown in Fig. 12(b). Moreover, a more compact SIW horn antenna without loading extended dielectric was proposed [29], as shown in Fig. 12(c). After detaching broad walls of SIW horn antenna, the left substrate not only acts as wave-guiding structure but also impedance transformer, which brings much size reduction and improves impedance matching simultaneously.

A ridged SIW (RSIW) horn antenna constructed by ten layers was designed [30]. Two layers were used to design coaxial feeding and the rest eight layers were used to design tapered ridge structure, as shown in Fig. 13. The bandwidth over 18–40 GHz was obtained while gain and radiation patterns were maintained across the bandwidth.

Based on the ridged SIW theory, a new ridged SIW horn antenna was implemented in a single substrate [31]. A three-step ridged SIW transition was realized by carving
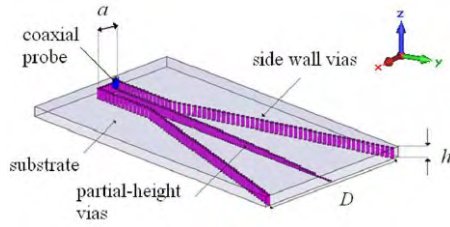
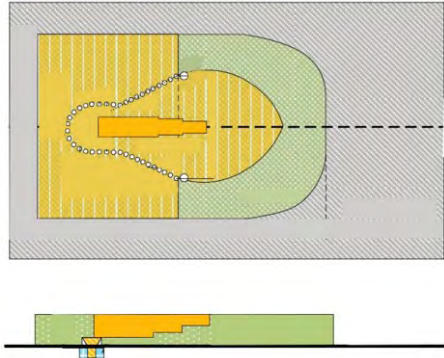**FIGURE 13.** Geometry of RSIW horn antenna with ten layers [30].

FIGURE 14. Geometry of single layer RSIW horn antenna [31].

FIGURE 15. Geometry of magnetoelectric dipole loaded SIW horn antenna and array [33].

FIGURE 16. Geometry of low-profile metamaterials-loaded SIW horn antenna [34].

a three-step groove with gold plating on the side and bottom walls of the substrate. Besides, an arc-shaped copper taper printed on the extended dielectric slab was loaded at horn aperture, as illustrated in Fig. 14. Finally, a wide bandwidth from 6.6 to 18 GHz was obtained. Furthermore, by etching slots along the sides of the flare part of above antenna, a slightly modified SIW horn antenna could be mounted on a large conducting cylinder with wider bandwidth [32].

A novel SIW end-fire magnetoelectric (ME) dipole antenna was proposed by Li and Luk [33]. It is observed that the low profile SIW antenna produces an ''8''-shaped radiation pattern in the H-plane, while an ''O''-shaped radiation pattern in the E-plane. The result proves that the radiating aperture can be viewed as an equivalent magnetic dipole in horizontal direction. Next, a metallic via was placed in front of the open-ended SIW aperture, which operated as an electric dipole in the vertical direction. Moreover, a pair of electric dipoles could improve the performance. Thus, SIW end-fire magnetoelectric dipole antenna was designed and fabricated, as shown in Fig. 15, and excellent radiation performances were obtained from measured results.

Through loading mushroom-type metamaterial in front of SIW horn aperture, much improvement in impedance bandwidth was achieved on a $1/20 \lambda_0$ thickness substrate [34], as shown in Fig. 16. Compared with previous SIW horn antennas, the proposed antenna realized the advantages of low profile and wide bandwidth.

To sum up, the comparison of different methods in improving bandwidth are concluded in Table 1. A series of representative methods are compared from the aspects of impedance bandwidth, substrate thickness, and number of layers. Every method owns distinct advantages as well as deficiency,
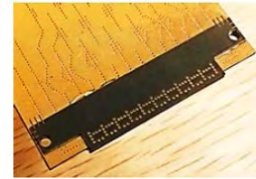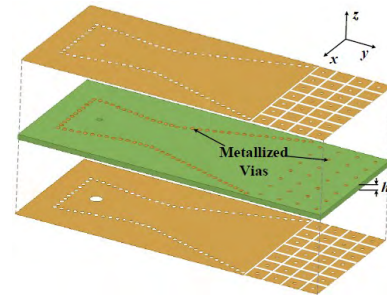
TABLE 1. Comparison of different methods in improving bandwidth.

Ref.	Impedance Bandwidth	Thickness	Number of Layers	Methods
[14]	5%	$0.225\lambda_0$	1	loading dielectric lens
[15]	10%	$0.24\lambda_0$	2	thick dielectric loading
[16]	6.4%	$0.36\lambda_0$	3	thin feeding network to thick horn transition by LTCC technology
[18]	16%	$0.10\lambda_0$	1	loading printed transition
[23]	40%	$0.18\lambda_0$	1	loading periodic parallel strips
[27]	40%	$0.33\lambda_0$	1	perforating air-vias
[30]	75%	$0.25\lambda_0$	10	employing ridged SIW structure
[33]	44%	$0.16\lambda_0$	3	loading magnetoelectric dipoles
[34]	10%	$0.05\lambda_0$	1	loading mushroom-type metamaterial

and it depends on the practical applications to choose a certain method.

B. HIGH GAIN SIW END-FIRE ANTENNAS

Fig. 17(a) shows a phase-corrected SIW horn antenna [35]. Three metal-via arrays were embedded inside the horn
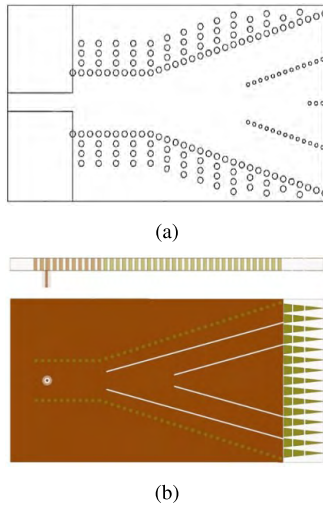
FIGURE 17. Geometry of phase corrected SIW horn antenna. (a) Example [35]. (b) Side view and top view of example [36].
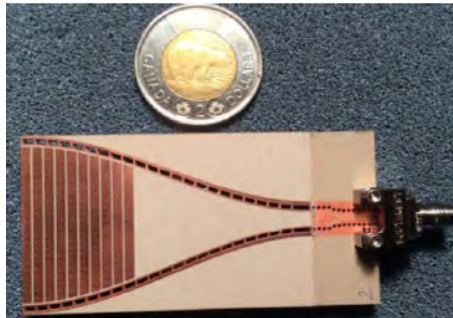

FIGURE 18. Geometry of SIW horn antenna loaded with hard and soft electromagnetic surfaces [37].
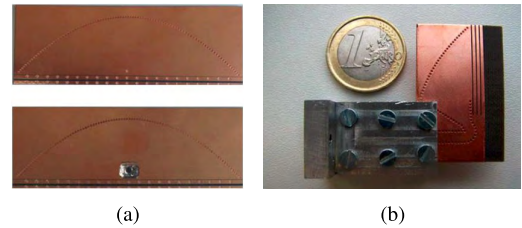

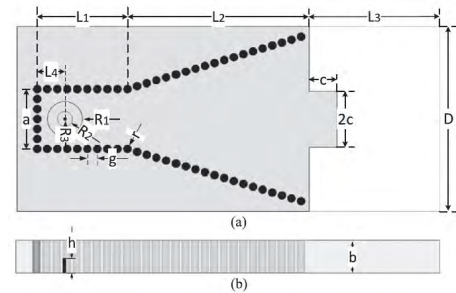FIGURE 19. Geometry of parabolic SIW horn antenna. (a) Example [39]. (b) Example [40].

FIGURE 20. Geometry of SIW horn antenna loaded with dielectric and small metal patch [41]. (a) Top view. (b) Side view.

resulting in nearly uniform phase distribution across the horn aperture. The gain of the proposed SIW antenna is 3.89 dB higher than the conventional one. Recently, this research group proposed a new gap SIW horn antenna to correct the phase distribution at the horn aperture [36]. The gap etched on the top and bottom of the antenna acted as magnetic wall so that the phase velocity could be controlled by modifying the position of the gap, as shown in Fig. 17(b). Uniform phase distribution was obtained and 2 dB gain improvement was realized.

By introducing hard and soft electromagnetic surfaces theory, Kishk proposed a new substrate integrated horn antenna with hard side walls combined with a couple of soft surfaces [37], as shown in Fig. 18. The uniform amplitude distribution and phase correction were realized due to the hard conditions, while the reduced back radiation was achieved due to the soft surfaces.

A dual band SIW H-plane horn antenna was designed in [38], and both broadside and end-fire radiation performances were achieved respectively. The gain of broadside radiation generated by etching slots reached to 8.87 dBi at 16.1 GHz, and the gain of end-fire radiation based on dielectric-loaded method was 11.3 dBi at 14.4 GHz.

A new large radiating aperture SIW horn antenna based on parabolic reflector principle was presented in [39] and [40], as shown in Fig. 19. Frontal feeding and offset feeding were adopted respectively and uniform phase distribution at the aperture was obtained. Thus, high gain SIW horn antenna was realized.

By improving front-to-back ratio of H-plane SIW horn antenna, high gain is realized. The conventional SIW horn antenna suffers high back-lobe radiation due to thin substrate. One of the methods was loading dielectric, on which a small rectangular metal patch was printed [41], as shown in Fig. 20. High gain performance was achieved thanks to the reduced sidelobes and backward radiation. Another one was employing a pair of slots, which were etched in the top and bottom metallization of the conventional SIW horn antenna [42]. A high gain of 10.4 dBi at 12.4 GHz was obtained with compact structure.

Besides, radiation performance of SIW horn antenna can be improved by empty SIW structure [43] or dual-ridged SIW structure [44].

All in all, the comparison of different methods in improving gain are concluded in Table 2. A series of representative methods are compared from the aspects of impedance bandwidth, center frequency, and corresponding gains. All the methods realize higher gain than the conventional method.

IV. CP SIW END-FIRE ANTENNAS

Due to attractive advantages of penetration in different climates, flexibility in alignment of the transmitter and receiver, reduction in multi-path interferences, circularly polarized antennas have been widely adopted in satellite communication, global positioning system (GPS), radar system, and etc. CP radiation is traditionally obtained by exciting

TABLE 2. Comparison of different methods in improving gain.

Ref.	Bandwidth	Center Frequency	Gain	Methods
[35]	20%	35.5 GHz	7.87 dBi	embedding metal via arrays
[36]	20%	34 GHz	10.3 dBi	employing gap SIW structure
[37]	10%	25 GHz	10.3 dBi	combining hard walls and soft surface
[40]	27%	31.5 GHz	15 dBi	employing parabolic reflector
[41]	2%	22.7 GHz	10.1 dBi	loading dielectric with a small metal patch
[42]	2%	12.4 GHz	10.4 dBi	employing a pair of slots

(a)   (b)
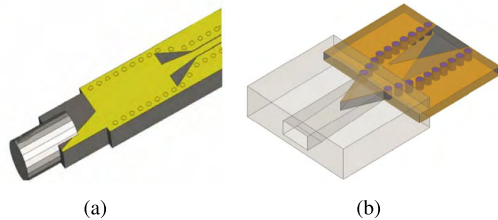
FIGURE 21. Geometry of circularly polarized ALTSA. (a) Example [47]. (b) Example [48].

two orthogonal modes with a 90° phase difference. Exciting horizontally polarized and vertically polarized electric field components simultaneously is one of requirements to generate circularly polarization. However, due to discontinuous metallized vias of SIW, the energy leakage results in weak propagation of horizontally polarized wave. Therefore, it is a great challenge for designing CP SIW end-fire antennas.

Inspired by the working principle of substrate integrated non-radiative dielectric (SINRD) guide [45], professor Mosig proposed a method that the propagation of both TE_{m0} and TE_{0n} modes was allowed simultaneously in SIW [46]. The permittivity difference on both sides of the metallic vias can be easily realized by drilling a periodic pattern of air holes, which can effectively prevent the energy leakage from via gaps. However, high permittivity substrate together with high complexity of optimization restrict its applications. Therefore, a series of researches emerge to design CP SIW end-fire antennas with simple structure and good performance.

Fig. 21(a) dipicts CP ALTSA designed on a thick substrate [47]. The vertically polarized wave generated by the SIW aperture together with the horizontally polarized wave generated by tapered slot result in circularly polarization. Moreover, a polystyrene rod was protruded from the edge of the tapered slot to increase its axial ratio (AR) bandwidth. Another CP ALTSA similar with the previous one was proposed in [48], as illustrated in Fig. 21(b). Wide AR bandwidth was obtained without loading dielectric rod.
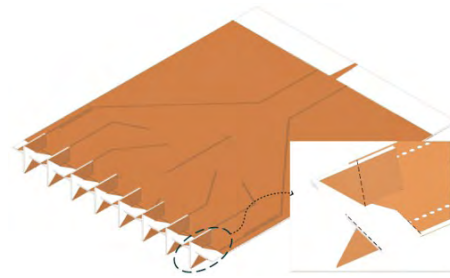
FIGURE 22. Geometry of circularly polarized ALTSA array [49].
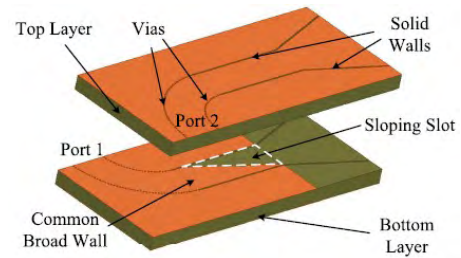
FIGURE 23. Geometry of dual circularly polarized SIW horn antenna [50].
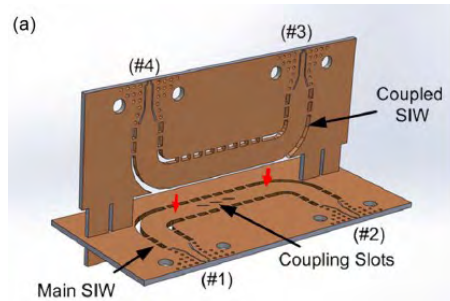
FIGURE 24. Geometry of three-dimensional 3-dB coupler [52].

Based on phase-corrected SIW horn antenna, Wang *et al.* [49] proposed effective methods to minimize the tapered length both for horizontally and vertically polarized linearly TSA arrays. Then, CP TSA array was designed by intersecting the HP and VP TSAs together, as shown in Fig. 22.

A compact wideband CP SIW horn antenna designed on two layers was proposed in [50], as shown in Fig. 23. A sloping slot etched on the common broad wall generated two orthogonal modes and phase shift. Thus, dual CP property could be realized from two different ports.

SIW with LEGO-like interconnected PCB building blocks was firstly proposed by Doghri *et al.* [51]. The coupling between broad wall and narrow wall results in rotation of electromagnetic wave. Finally, CP SIW end-fire antennas can be realized when three-dimensional 3-dB coupler is adopted as feeding network [52], [53], as illustrated in Fig. 24.

A high gain SIW H-plane horn antenna and a vivaldi antenna were combined to produce two orthogonal polarizations on a single substrate, resulting in circularly polarized endfire radiation [54]. The measured results showed that the proposed antenna operated with a wideband from
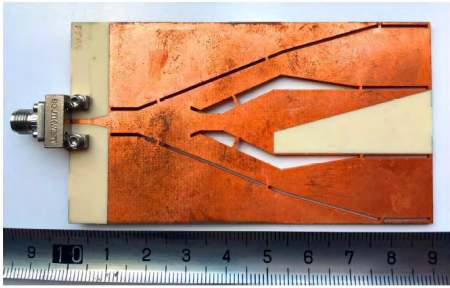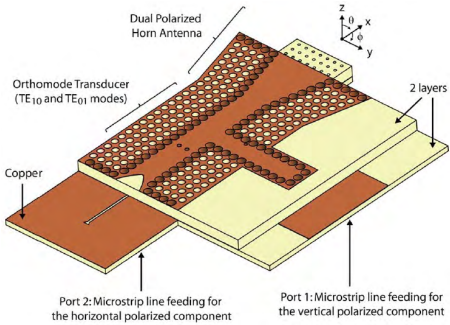
FIGURE 25. The prototype of CP antenna [55].

FIGURE 26. Geometry of dual-polarized SIW horn antenna [56].

FIGURE 27. Geometry of the proposed dual-polarized horn antenna, OMT, and feeding ports [57].

| (a) | (b) |

FIGURE 28. Prototype of the proposed multibeam dual-circularly polarized antenna array [58]. (a) Top view. (b) Bottom view.

TABLE 3. Comparison of different methods of circularly polarized end-fire antennas.

Ref.	AR Bandwidth	Impedance Bandwidth	Thickness	Methods
[47]	14%	29%	$0.21\lambda_0$	SIW fed tapered slot antenna
[48]	34.7%	31.5%	$0.25\lambda_0$	SIW fed tapered slot antenna
[49]	3.1%	6%	$0.017\lambda_0$	combining cross-LTSAs
[50]	11.8%	> 26%	$0.5\lambda_0$	etching sloping slot on the common broad wall
[54]	9%	> 20%	$0.13\lambda_0$	combining SIW H-plane horn antenna and a vivaldi antenna
[55]	5.9%	5%	$0.12\lambda_0$	integrating phase controlling and power dividing structure

24.25 to 26.5 GHz, with a high and uniform gain of almost 8 dB.

By employing an integrated phase controlling and power dividing structure, two orthogonal electric fields with identical amplitude and 90° phase difference were achieved, leading to circular polarization on a single-layer substrate [55]. The measured results indicated a 5% bandwidth was obtained with the gain of 8.5 dBi. The prototype of the proposed antenna is depicted in Fig. 25.

Due to the extended substrate integrated waveguide (ESIW), both TE_{m0} and TE_{0n} modes were realized simultaneously inside SIW [46]. As illustrated in Fig. 26, a dual-polarized horn antenna based on ESIW technology was presented in [56], which was fed by an orthomode transducer (OMT) on two layers of substrate. Two orthogonal modes, TE_{10} and TE_{01}, were firstly combined in a substrate integrated structure, leading to a dual-polarized horn antenna. Besides, the proposed horn antenna exhibited a bandwidth of 8.6% with good isolation between two modes.

An E-band SIW dual-polarized horn antenna was proposed in [57], which was fed by an OMT on two layers of substrate as well. As depicted in Fig. 27, port 1 is an SIW section to excite TE_{10} mode for the vertical polarization, while port 2 is a quasi-coaxial stripline to excite quasi-TEM mode for the horizontal polarization. Thus, a dual-polarized horn antenna with frequency bandwidth from 83 GHz to 87 GHz was achieved.

By etching stepped slot at the middle metallic layer between the two dielectric layers, a dual-CP end-fire antenna element was designed for broadband millimeter wave applications [58]. What's more, the additional dielectric was loaded in front of the radiation aperture to improve the
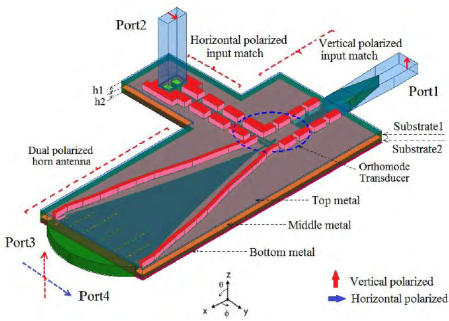
interelement isolation and radiation performance. As shown in Fig. 28, a broadband multibeam antenna array was designed and fabricated, which realized wide impedance bandwidth of 29.3% and AR bandwidth of 22.5%.

All in all, the comparison of different methods of circularly polarized end-fire antennas are concluded in Table 3. A series of representative methods are compared from the aspects of AR bandwidth, impedance bandwidth, substrate thickness.

V. CONCLUSION

With the development of 5G communication, the operating frequency goes high to higher than 20 GHz, in which SIW end-fire antennas are very easy in design, compact in size,

cost effective in manufacturing and easy for integration. Also they are suitable for array design for beamscanning and other beamforming systems in PCBs. SIW end-fire antennas and their applications are considered to be an attractive research area in wireless communications. This paper briefly reviews the recent development of SIW end-fire antennas. Aiming at challenges encountered in studies, we focus on the design of VP and CP SIW end-fire antennas in this paper. Many different antenna examples are presented. In design of VP antennas, most of the methods resulted in significant improvement in impedance bandwidth and radiation gains. In design of CP antennas, several novel methods are proposed and detailed analyses are presented. Moreover, the design of antenna array is also involved in this paper, which accelerates the practical process of SIW end-fire antennas. We are looking forward to observing more engineering applications of these antennas in the near future.

Current microwave and millimeter-wave research in connection with SIW end-fire antennas suggests the following future trends.

1) Research on the step-changed equivalent dielectric constant of the substrate with low profile, which will extend its applications in antenna design area. Under Ka band, commercial substrate can't realize the effect of step-changed equivalent dielectric constant, which constraints operating band of SIW end-fire antennas. Besides, the design of feeding network is also a challenge. It is necessary to control the equivalent dielectric constant of the substrate flexibly. Moreover, impedance mismatch is a common issue in antenna design, such as the design of microstrip antennas. Therefore, substrate with step-changed equivalent dielectric constant can be adopted in more practical applications.

2) Research on dual circularly polarized SIW end-fire antenna array. Dual CP SIW end-fire antennas and CP end-fire antenna arrays have been studied and designed by researchers. However, it is a challenge to design dual CP SIW end-fire antenna array which attracts much attention for its expansive applications. Fortunately, based on the various methods of designing dual CP SIW end-fire antennas and CP SIW end-fire antenna arrays, the new method of realizing dual CP SIW end-fire antenna array is on the way.

3) The corrugated substrate integrated waveguide (CSIW) uses quarter wavelength microstrip stubs instead of metallized-vias to achieve TE_{10} type boundary conditions at the side walls [59], [60]. Due to the isolated conductors, CSIW permits shunt connection with other active devices. Based on CSIW, antennas have been presented in [61] and [62], which achieved good performances, such as wide bandwidth and low side lobe level. Besides, the CSIW could reduce the antenna size and fabrication cost because of no vias. Therefore, CSIW is a promising technology.

REFERENCES

[1] R. E. Collin and F. J. Zucker, *Antenna Theory Part 2*. New York, NY, USA: McGraw-Hill, 1969.

[2] P. S. Excell, A. D. Tinniswood, and R. W. Clarke, "Log-periodic antenna for pulsed radiation," *Electron. Lett.*, vol. 34, no. 21, pp. 1990–1991, Oct. 1998.

[3] F. Zhang, F.-S. Zhang, G. Zhao, C. Lin, and Y.-C. Jiao, "A loaded wideband linearly tapered slot antenna with broad beamwidth," *IEEE Antennas Wireless Propag. Lett.*, vol. 10, pp. 79–82, 2011.

[4] E. A. Jones and W. T. Joines, "Design of Yagi-Uda antennas using genetic algorithms," *IEEE Trans. Antennas Propag.*, vol. 45, no. 9, pp. 1386–1392, Sep. 1997.

[5] Z. C. Hao, W. Hong, J. X. Chen, X. P. Chen, and K. Wu, "A novel feeding technique for antipodal linearly tapered slot antenna array," in *IEEE MTT-S Int. Microw. Symp. Dig.*, Jun. 2005, pp. 1641–1643.

[6] Y. J. Cheng, W. Hong, and K. Wu, "Design of a monopulse antenna using a dual V-type linearly tapered slot antenna (DVLTSA)," *IEEE Trans. Antennas Propag.*, vol. 56, no. 9, pp. 2903–2909, Sep. 2008.

[7] Y. J. Cheng and Y. Fan, "Millimeter-wave miniaturized substrate integrated multibeam antenna," *IEEE Trans. Antennas Propag.*, vol. 59, no. 12, pp. 4840–4844, Dec. 2011.

[8] X. Y. Wu and P. S. Hall, "Substrate integrated waveguide Yagi-Uda antenna," *Electron. Lett.*, vol. 46, no. 23, pp. 1541–1542, 2010.

[9] X. Zou, C.-M. Tong, J.-S. Bao, and W.-J. Pang, "SIW-fed Yagi antenna and its application on monopulse antenna," *IEEE Antennas Wireless Propag. Lett.*, vol. 13, pp. 1035–1038, 2014.

[10] G. H. Zhai, W. Hong, K. Wu, and Z. Q. Kuai, "Wideband substrate integrated printed log-periodic dipole array antenna," *IET Microw. Antennas Propag.*, vol. 4, no. 7, pp. 899–905, Jul. 2010.

[11] M. Clénet, J. Litzenberger, D. Lee, S. Thirakoune, G. A. Morin, and Y. M. M. Antar, "Laminated waveguide as radiating element for array applications," *IEEE Trans. Antennas Propag.*, vol. 54, no. 5, pp. 1481–1487, May 2006.

[12] Z. Li, K. Wu, and T. A. Denidni, "A new approach to integrated horn antenna," in *Proc. 10th Int. Symp. Antenna Technol. Appl. Electromagn.*, Jul. 2004, pp. 1–3.

[13] B. Pan, Y. Li, G. E. Ponchak, J. Papapolymerou, and M. M. Tentzeris, "A 60-GHz CPW-fed high-gain and broadband integrated horn antenna," *IEEE Trans. Antennas Propag.*, vol. 57, no. 4, pp. 1050–1056, Apr. 2009.

[14] H. Wang, D.-G. Fang, B. Zhang, and W.-Q. Che, "Dielectric loaded substrate integrated waveguide (SIW) H-plane horn antennas," *IEEE Trans. Antennas Propag.*, vol. 58, no. 3, pp. 640–647, Mar. 2010.

[15] M. Yousefbeiki, A. A. Domenech, J. R. Mosig, and C. A. Fernandes, "Ku-band dielectric-loaded SIW horn for vertically-polarized multi-sector antennas," in *Proc. 6th Eur. Conf. Antennas Propag. (EUCAP)*, Mar. 2012, pp. 2367–2371.

[16] S. B. Yeap, X. Qing, M. Sun, and Z. N. Chen, "140-GHz 2×2 SIW horn array on LTCC," in *Proc. IEEE Asia–Pacific Conf. Antennas Propag.*, Aug. 2012, pp. 279–280.

[17] Y. Lang and S.-W. Qu, "A dielectric loaded H-plane horn for millimeter waves based on LTCC technology," in *Proc. Cross Strait Quad-Regional Radio Sci. Wireless Technol. Conf. (CSQRWC)*, Jul. 2013, pp. 265–268.

[18] M. Esquius-Morote, B. Fuchs, J. F. Zürcher, and J. R. Mosig, "A printed transition for matching improvement of SIW horn antennas," *IEEE Trans. Antennas Propag.*, vol. AP-61, no. 4, pp. 1923–1930, Apr. 2013.

[19] M. Esquius-Morote, B. Fuchs, J. Zurcher, and J. R. Mosig, "Novel thin and compact H-plane SIW horn antenna," *IEEE Trans. Antennas Propag.*, vol. 61, no. 6, pp. 2911–2920, Jun. 2013.

[20] M. Esquius-Morote, J. Zürcher, J. R. Mosig, and B. Fuchs, "Low-profile direction finding system with SIW horn antennas for vehicular applications," in *Proc. IEEE Antennas Propag. Soc. Int. Symp. (APSURSI)*, Jul. 2014, pp. 591–592.

[21] H. Xu, Y. Li, D. Ye, and Y. Long, "A broadband offset-parallel-parallelograms printed endfire antenna," *IEEE Antennas Wireless Propag. Lett.*, vol. 16, pp. 1167–1170, 2017.

[22] Y. Cao, Y. Cai, C. Jin, Z. Qian, L. Zhu, and W. Zhang, "Broadband SIW horn antenna loaded with offset double-sided parallel-strip lines," *IEEE Antennas Wireless Propag. Lett.*, vol. 17, no. 9, pp. 1740–1744, Sep. 2018.

[23] L. Wang, M. Garcia-Vigueras, M. Alvarez-Folgueiras, and J. R. Mosig, "Wideband H-plane dielectric horn antenna," *IET Microw., Antennas Propag.*, vol. 11, no. 12, pp. 1695–1701, Sep. 2017.

[24] L. Wang, M. Garcia-Vigueras, and J. R. Mosig, "Matching and gain enhancement of leaky-wave dielectric horn antenna," in *Proc. 10th Eur. Conf. Antennas Propag. (EuCAP)*, Davos, Switzerland, Apr. 2016, pp. 1–4.

[25] Y. Tang, Z. Wang, L. Xia, and P. Chen, "A novel high gain K-band H-plane SIW horn antenna using dielectric loading," in *Proc. Asia–Pacific Microw. Conf. (APMC)*, Nov. 2014, pp. 372–374.

[26] J. Puskely, T. Urbanec, T. Mikulasek, Z. Raida, V. Rericha, and J. Bartyzal, "Novel planar horn antenna for 75/85 GHz experimental wireless link," *Radioengineering*, vol. 24, no. 3, pp. 681–687, 2015.

[27] Y. Cai, Z.-P. Qian, Y.-S. Zhang, J. Jin, and W.-Q. Cao, "Bandwidth enhancement of SIW horn antenna loaded with air-via perforated dielectric slab," *IEEE Antennas Wireless Propag. Lett.*, vol. 13, pp. 571–574, 2014.

[28] Y. Cai *et al.*, "Compact wideband SIW horn antenna fed by elevated-CPW structure," *IEEE Trans. Antennas Propag.*, vol. 63, no. 10, pp. 4551–4557, Oct. 2015.

[29] Y. Cai, Y. Zhang, Z. Qian, W. Cao, and L. Wang, "Design of compact air-vias-perforated SIW horn antenna with partially detached broad walls," *IEEE Trans. Antennas Propag.*, vol. 64, no. 6, pp. 2100–2107, Jun. 2016.

[30] A. R. Mallahzadeh and S. Esfandiarpour, "Wideband H-plane horn antenna based on ridge substrate integrated waveguide (RSIW)," *IEEE Antennas Wireless Propag. Lett.*, vol. 11, pp. 85–88, 2012.

[31] Y. Zhao, Z. Shen, and W. Wu, "Wideband and low-profile H-plane ridged SIW horn antenna mounted on a large conducting plane," *IEEE Trans. Antennas Propag.*, vol. 62, no. 11, pp. 5895–5900, Nov. 2014.

[32] Y. Zhao, Z. Shen, and W. Wu, "Conformal SIW H-plane horn antenna on a conducting cylinder," *IEEE Antennas Wireless Propag. Lett.*, vol. 14, pp. 1271–1274, 2015.

[33] Y. Li and K.-M. Luk, "A multibeam end-fire magnetoelectric dipole antenna array for millimeter-wave applications," *IEEE Trans. Antennas Propag.*, vol. 64, no. 7, pp. 2894–2904, Jul. 2016.

[34] Y. Cai, Y. Zhang, L. Yang, Y. Cao, and Z. Qian, "Design of low-profile metamaterial-loaded substrate integrated waveguide horn antenna and its array applications," *IEEE Trans. Antennas Propag.*, vol. 65, no. 7, pp. 3732–3737, Jul. 2017.

[35] L. Wang, X. Yin, S. Li, H. Zhao, L. Liu, and M. Zhang, "Phase corrected substrate integrated waveguide H-plane horn antenna with embedded metal-via arrays," *IEEE Trans. Antennas Propag.*, vol. 62, no. 4, pp. 1854–1861, Apr. 2014.

[36] L. Wang, M. Esquius-Morote, H. Qi, X. Yin, and J. R. Mosig, "Phase corrected *H*-plane horn antenna in gap SIW technology," *IEEE Trans. Antennas Propag.*, vol. 65, no. 1, pp. 347–353, Jan. 2017.

[37] N. Bayat-Makou and A. A. Kishk, "Substrate integrated horn antenna with uniform aperture distribution," *IEEE Trans. Antennas Propag.*, vol. 65, no. 2, pp. 514–520, Feb. 2017.

[38] T. Agrawal and S. Srivastava, "Ku band pattern reconfigurable substrate integrated waveguide leaky wave horn antenna," *AEU—Int. J. Electron. Commun.*, vol. 87, pp. 70–75, Apr. 2018.

[39] S. Zhang, Z. Li, and J. Wang, "A novel SIW H-plane horn antenna based on parabolic reflector," *Int. J. Antennas Propag.*, vol. 2016, Jun. 2016, Art. no. 3659230.

[40] J. Lambor, J. Lacik, Z. Raida, and H. Arthaber, "High-gain wideband SIW offset parabolic antenna," *Microw. Opt. Technol. Lett.*, vol. 58, no. 12, pp. 2888–2892, 2016.

[41] L. Gong, K. Y. Chan, and R. Ramer, "Substrate integrated waveguide H-plane horn antenna with improved front-to-back ratio and reduced sidelobe level," *IEEE Antennas Wireless Propag. Lett.*, vol. 15, pp. 1835–1838, 2016.

[42] Y. Luo and J. Bornemann, "Substrate integrated waveguide horn antenna on thin substrate with back-lobe suppression and its application to arrays," *IEEE Antennas Wireless Propag. Lett.*, vol. 16, pp. 2622–2625, 2017.

[43] J. Mateo, A. M. Torres, A. Belenguer, and A. L. Borja, "Highly efficient and well-matched empty substrate integrated waveguide H-plane horn antenna," *IEEE Antennas Wireless Propag. Lett.*, vol. 15, pp. 1510–1513, 2016.

[44] J. Li *et al.*, "Wideband *SIWH*-plane dual-ridged end-fire antenna for conformal application," *Microw. Opt. Technol. Lett.*, vol. 59, no. 2, pp. 286–292, 2017.

[45] Y. Cassivi and K. Wu, "Substrate integrated nonradiative dielectric waveguide," *IEEE Microw. Wireless Compon. Lett.*, vol. 14, no. 3, pp. 89–91, Mar. 2004.

[46] M. Esquius-Morote *et al.*, "Extended SIW for TE_{m0} and TE_{0n} modes and slotline excitation of the TE_{01} mode," *IEEE Microw. Wireless Compon. Lett.*, vol. 23, no. 8, pp. 412–414, Aug. 2013.

[47] S. Lin, A. Elsherbini, S. Yang, A. Fathy, A. Kamel, and H. Elhennawy, "Experimental development of a circularly polarized antipodal tapered slot antenna using SIW feed printed on thick substrate," in *Proc. IEEE Antennas Propag. Soc. Int. Symp.*, Jun. 2007, p. 1533—1536.

[48] X. Cheng, Y. Yao, J. Yu, and X. Chen, "Circularly polarized substrate-integrated waveguide tapered slot antenna for millimeter-wave applications," *IEEE Antennas Wireless Propag. Lett.*, vol. 16, pp. 2358–2361, 2017.

[49] L. Wang, X. Yin, M. Esquius-Morote, H. Zhao, and J. R. Mosig, "Circularly polarized compact LTSA array in SIW technology," *IEEE Trans. Antennas Propag.*, vol. 65, no. 6, pp. 3247–3252, Jun. 2017.

[50] Y. Cai, Y. Zhang, Z. Qian, W. Cao, and S. Shi, "Compact wideband dual circularly polarized substrate integrated waveguide horn antenna," *IEEE Trans. Antennas Propag.*, vol. 64, no. 7, pp. 3184–3189, Jul. 2016.

[51] A. Doghri, T. Djerafi, A. Ghiotto, and K. Wu, "SIW 90-degree twist for substrate integrated circuits and systems," in *IEEE MTT-S Int. Microw. Symp. Dig.*, Jun. 2013, pp. 1–3.

[52] A. Doghri, T. Djerafi, A. Ghiotto, and K. Wu, "Substrate integrated waveguide directional couplers for compact three-dimensional integrated circuits," *IEEE Trans. Microw. Theory Techn.*, vol. 63, no. 1, pp. 209–221, Jan. 2015.

[53] T. Djerafi, B. Youzkatli-el-Khatib, K. Wu, and S. O. Tatu, "Substrate integrated waveguide antenna subarray for broadband circularly polarised radiation," *IET Microw., Antennas Propag.*, vol. 8, no. 14, pp. 1179–1185, 2014.

[54] S. S. Hesari and J. Bornemann, "Wideband circularly polarized substrate integrated waveguide endfire antenna system with high gain," *IEEE Antennas Wireless Propag. Lett.*, vol. 16, pp. 2262–2265, 2017.

[55] Y. Yin, B. Zarghooni, and K. Wu, "Single-layered circularly polarized substrate-integrated waveguide horn antenna array," *IEEE Trans. Antennas Propag.*, vol. 65, no. 11, pp. 6161–6166, Nov. 2017.

[56] M. Esquius-Morote, M. Mattes, and J. R. Mosig, "Orthomode transducer and dual-polarized horn antenna in substrate integrated technology," *IEEE Trans. Antennas Propag.*, vol. 62, no. 10, pp. 4935–4944, Oct. 2014.

[57] H. Jin, Y. M. Huang, H. Jin, and K. Wu, "*E*-band substrate integrated waveguide orthomode transducer integrated with dual-polarized horn antenna," *IEEE Trans. Antennas Propag.*, vol. 66, no. 5, pp. 2291–2298, May 2018.

[58] Q. Wu, J. Hirokawa, J. Yin, C. Yu, H. Wang, and W. Hong, "Millimeter-wave multibeam endfire dual-circularly polarized antenna array for 5G wireless applications," *IEEE Trans. Antennas Propag.*, vol. 66, no. 9, pp. 4930–4935, Sep. 2018.

[59] K. W. Eccleston, "Mode analysis of the corrugated substrate integrated waveguide," *IEEE Trans. Microw. Theory Techn.*, vol. 60, no. 10, pp. 3004–3012, Oct. 2012.

[60] D. G. Chen and K. W. Eccleston, "Substrate integrated waveguide with corrugated wall," in *Proc. Asia–Pacific Microw. Conf.*, Dec. 2008, pp. 1–4.

[61] T. Djerafi and K. Wu, "Corrugated substrate integrated waveguide (SIW) antipodal linearly tapered slot antenna array fed by quasi-triangular power divider," *Prog. Electromagn. Res. C*, vol. 26, pp. 139–151, Dec. 2012.

[62] S. Ranade, A. Majumder, and S. Chatterjee, "Corrugated substrate integrated waveguide fed broadband tapered slot antenna at Ku band," in *Proc. IEEE Appl. Electromagn. Conf. (AEMC)*, Dec. 2015, pp. 1–2.

YUFAN CAO was born in Qingzhou, Shandong, China, in 1990. He received the B.S. and M.S. degrees in communication engineering from the PLA University of Science and Technology, Nanjing, China, in 2013 and 2016, respectively.

His research interests include microstrip patch antennas, substrate-integrated waveguide antennas, and horn antennas.

YANG CAI was born in Suzhou, Anhui, China, in 1991. He received the B.S. degree in communication engineering from the PLA University of Science and Technology, Nanjing, China, in 2012, and the Ph.D. degree in electronics science and technology from Army Engineering University, Nanjing, China, in 2017.

Since 2017, he has been with Space Engineering University, Beijing, China, as a Lecturer. His research interests include substrate-integrated waveguide antennas, horn antennas, metamaterials, and their applications to antennas.
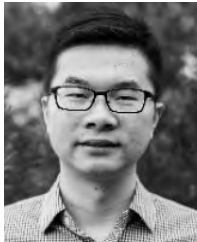
LEI WANG (S'09–M'16) received the Ph.D. degree in electromagnetic field and microwave technology from Southeast University, Nanjing, China, in 2015. From 2014 to 2016, he was a Research Fellow and held a post-doctoral position with the Laboratory of Electromagnetics and Antennas, Swiss Federal Institute of Technology, Lausanne, Switzerland. From 2016 to 2017, he was a Post-Doctoral Research Fellow with the Electromagnetic Engineering Laboratory, KTH Royal Institute of Technology, Stockholm, Sweden. Since 2017, he has been an Alexander von Humboldt Scholar with the Institute of Electromagnetic Theory, Hamburg University of Technology, Hamburg, Germany. His research includes the antenna theory and applications, active electronically scanning arrays, integrated antennas and arrays, substrate-integrated waveguide antennas, leaky-wave antennas, horn antennas, numerical modeling and optimization of small antennas, and wireless propagations.

He received the Chinese National Scholarship for Ph.D. Candidates in 2014. He was also granted the Swiss Government Excellence Scholarship to conduct research on SIW horn antennas and applications in 2014. He was granted the Alexander von Humboldt Research Foundation to take research on antenna modeling and optimization in 2016. He received the Best Poster Award in the 2018 IEEE International Workshop on Antenna Technology.

ZUPING QIAN (M'01) was born in Haimen, Jiangsu, China, in 1961. He received the B.S. and M.S. degrees in applied mathematics from Hunan University, Changsha, China, in 1982 and 1985, respectively, and the Ph.D. degree in microwave techniques from Southeast University, Nanjing, China, in 2000.

During 1985 to 1999, he was with the Institute of Communications Engineering, Nanjing, as a Lecturer and later as an Associate Professor. From 2000 to 2017, he was a Professor with the College of Communications Engineering, PLA University of Science and Technology, Nanjing. Since 2017, he has been a Professor with the College of Communications Engineering, Army Engineering University of PLA, Nanjing. He has authored or co-authored more than 80 international and regional refereed journal papers. His research interests include antenna, metamaterials, computational electromagnetics, array signal processing, and EMI/EMC.

LEI ZHU received the B.Sc., M.Sc., and Ph.D. degrees from the College of Communications Engineering, PLA University of Science and Technology, China, in 1996, 1999, and 2002, respectively.

He is currently a Professor of the Army Engineering University of PLA. His research interests are network planning, data analysis, and system simulation.

• • •